electronics

Article

Regularized Zero-Forcing Dirty Paper Precoding in a High-Throughput Satellite Communication System

Mingchuan Yang *, Xinye Shao, Guanchang Xue, Botao Liu and Yanyong Su

Communication Research Center, Harbin Institute of Technology, Harbin 150001, China
* Correspondence: mcyang@hit.edu.cn

Abstract: In order to maximize the available data rate and spectrum utilization efficiency, a high-throughput satellite communication system adopts the full spectrum reuse scheme, which will cause serious co-frequency interference. In this paper, a forward link model, considering the effects of free space loss, rainfall attenuation, and beam gain, is established, and the classical low-complexity of the zero-forcing precoding algorithm is improved in order to solve the serious co-frequency interference. Moreover, the regularized zero-forcing precoding algorithm considering the influence of system noise is studied, and a low complexity regularized zero-forcing dirty paper precoding algorithm is proposed, whose basic principle is to sort users based on the principle of channel maximum norm selection and practical application scenarios. Simulation results show that it can encode users sequentially, according to the channel conditions, to maximize the SINR (signal-to-interference-plus-noise ratio) and increase the throughput of the system.

Keywords: high-throughput satellite; full spectrum reuse; co-frequency interference; precoding; zero-forcing precoding

Citation: Yang, M.; Shao, X.; Xue, G.; Liu, B.; Su, Y. Regularized Zero-Forcing Dirty Paper Precoding in a High-Throughput Satellite Communication System. *Electronics* **2022**, *11*, 3106. https://doi.org/10.3390/electronics11193106

Academic Editor: Athanasios D. Panagopoulos

Received: 15 September 2022
Accepted: 26 September 2022
Published: 28 September 2022

1. Introduction

With the development of the global mobile Internet and the "ubiquitous" network demand of individual consumers, a high-throughput satellite communication system with the characteristics of "operating in high frequency band, high throughput and providing broadband Internet access service" is the development trend [1]. With the same spectrum resources, high-throughput satellites can obtain several times the communication capacity than that of fixed satellites by using multi-beam and frequency reuse technology. On the premise of maximizing the available data rate and spectrum utilization efficiency, high-throughput satellites have adopted the full spectrum reuse scheme, which will cause serious co-frequency interference. Precoding technology is an effective method to deal with this problem. The principle of precoding technology is to complete signal processing according to channel state information, so as to mitigate interference and improve link performance. Precoding technology is generally applied to the downlink channel of the forward link of high-throughput satellites.

Precoding technology is mainly divided into linear and nonlinear precoding technology. Although traditional nonlinear precoding can achieve better performance, it is difficult to apply in practice due to its high complexity, such as the use of dirty paper coding which, can achieve the optimal capacity [2]. However, linear precoding has received extensive attention in the academic community due to its relatively low complexity. The classical zero-forcing precoding algorithm [3] in linear precoding was first applied to high-throughput satellites by Cottatellucci and Debbah [4]. It has been proven that linear precoding technology can effectively improve the communication capacity performance of the system. At the same time, the influence of channel estimation error, feedback delay, and on-board payload on the overall system performance is also studied and analyzed. Subsequently, reference [5] focuses on the performance of spectrum utilization when a

Ka-band high-throughput satellite system adopts regularized zero-forcing linear precoding, and studies the terrestrial user grouping service under the practical constraints of channel state information delay and oscillator phase noise. On this basis, reference [6] reasonably applies nonlinear dirty paper coding technology in a high-throughput satellite system based on the DVB-S2 standard, and compares it with linear methods such as zero-forcing and regularized zero-forcing. They provide the performance upper limit of the multi-beam joint precoding method, and verify the relationship between beam coverage parameters and system communication capacity. Reference [7] proposes a real-time demonstration of precoding technology, which is used to realize full spectrum reuse in the forward link of a future high-throughput satellite system, proving the feasibility of precoding in satellite communications based on the superframe structure defined in DVB-S2X standard. Reference [8] designs a zero-forcing precoder using partial channel state information for matrix and vector normalization, which can reduce the delay and signaling overhead by reducing the channel state information feedback from the user terminal. Reference [9] summarizes the latest precoding technology for a high-throughput satellite system, and points out its future development direction and challenges. Reference [10] surveys the alternative fade mitigation techniques for satellite communication systems operating at Ku, Ka, and V frequency bands. The specific phenomena influencing the propagation of radio waves on Earth-space links are also overviewed. Reference [11] performs a detailed prognostic evaluation of radio wave propagation attenuation due to rain, free space, gases, and clouds over the atmosphere at the ultra-high frequency band by employing relevant empirical atmospheric data and suitable propagation models for robust prognostic modeling using experimental measurements. Reference [12] proposes a complete model of atmospheric propagation to improve the estimation and the analysis of atmospheric effects on the signal quality in satellite communications using actual measured parameters.

Although the current research on the precoding technology of high-throughput satellite systems has made great progress, the improvement in SINR (signal-to-interference-plus-noise ratio) is still insufficient, and there is still a gap regarding the throughput requirements of high-throughput satellites. Therefore, further research and improvement of high-throughput satellite precoding technology are still needed in order to continue to optimize the SINR.

Based on the above research and analyses, after establishing the forward link model considering the effects of free space loss, rainfall attenuation, and beam gain, this paper improves the classical low-complexity zero-forcing precoding algorithm and studies the regularized zero-forcing precoding algorithm, considering the influence of system noise. Based on the idea of dirty paper coding, a low complexity dirty paper regularized zero-forcing precoding algorithm is proposed in this paper, which aims to encode users sequentially according to the channel conditions to maximize the SINR and increase the throughput of the system. The remainder of the paper is organized as follows. Section 2 describes the system architecture and channel model. The regularized zero-forcing dirty paper precoding of a high-throughput satellite communication system is given in Section 3. The simulation results and analysis are presented in Section 4, followed by the conclusion in Section 5.

2. High-Throughput Satellite Communication System Model

2.1. High-Throughput Satellite Communication System Architecture

The high-throughput satellite communication system is divided into three main segments: the ground segment, the space segment, and the user segment. All the user terminals covered by all the spot beams of the satellite constitute the user segment. The ground segment is mainly composed of gateway stations, which are responsible for sending signals to and receiving signals from satellites. The space segment includes the satellites and all the ground facilities for monitoring and controlling them. The definition of the link between different segments of the high-throughput satellite communication system is different. The feeder link is the wireless link connecting the satellite and the gateway station, and the user link is the link connecting the user terminal and the satellite. The forward uplink from

the gateway station to the satellite and the forward downlink from the satellite to the user constitute the forward link of the high-throughput satellite system. The reverse uplink from the user to the satellite and the reverse downlink from the satellite to the gateway station constitute the reverse link of the high-throughput satellite system, which is shown in Figure 1.

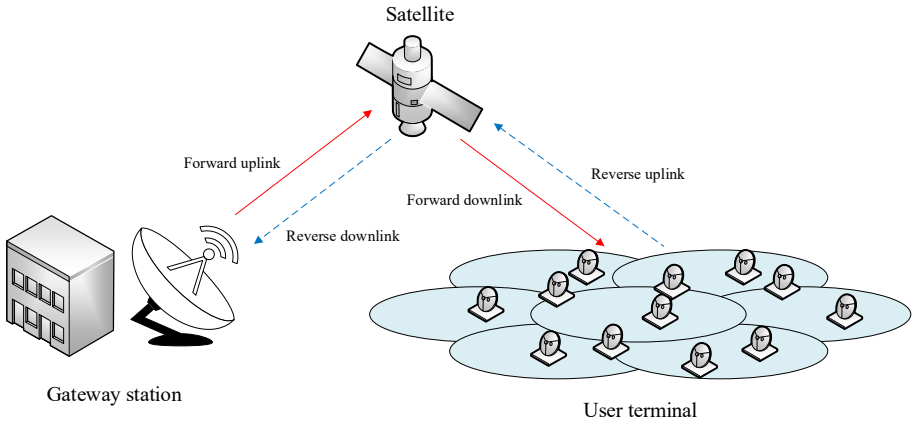

Figure 1. Forward link and reverse link of high-throughput satellite system.

2.2. High-Throughput Satellite Communication System Signal Model

The forward link of high-throughput satellite system transmits independent information streams to multiple fixed terminals through multiple beams. The scenario of a single gateway station with a single feed per beam is studied in this paper, in which a gateway station manages adjacent beams with full spectrum reuse by controlling feeds on the satellite. However, full spectrum reuse will bring serious co-frequency interference; that is, at the same time, users in each beam will receive interference from users in other beams when receiving their own signals. The system adopts a time division multiplexing scheme, in which each beam provides service for only one user in each time slot. The schematic diagram of the forward link of a high-throughput satellite communication system is shown in Figure 2.

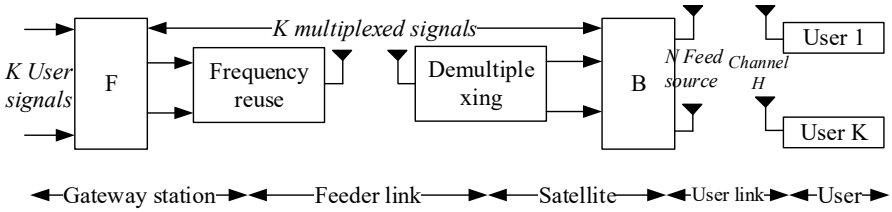

Figure 2. Schematic diagram of the forward link of a high-throughput satellite communication system.

Suppose that the i-th user signal sent by the ground gateway can be expressed as s_i. For any user signal s_i sent to K beams, its average power is 1; that is, $E[s_i^2] = 1, \forall i = 1, 2 \cdots K$. Suppose that the precoding vector is $\mathbf{t}_i = \sqrt{p_i}\mathbf{w}_i$, where $p_i = \left\|\mathbf{t}_i^2\right\|$ is the signal power of the i-th user and $\mathbf{w}_i = \frac{\mathbf{t}_i}{\|\mathbf{t}_i\|}$ is the normalized precoding vector. The onboard transmitted signal is the superposition of all beam signals, i.e., $\sum_{i=1}^{K} \mathbf{t}_i s_i$. The received signal of user i can be expressed as:

$$y_i = \mathbf{h}_i^H \mathbf{t}_i s_i + \mathbf{h}_i^H \sum_{j=1.j\neq i}^{K} \mathbf{t}_j s_j + n_i \quad (1)$$

where the first term is the useful signal, the second term is the interference signal, and the third term n_i is zero-mean Gaussian random noise with independent identical distribution.

$\mathbf{h}_i = \mathbf{b}_i\mathbf{d}_i$ is $N \times 1$ dimension channel matrix, where $\mathbf{b}_i$ is multi-beam gain, and $\mathbf{d}_i$ is logarithmic random attenuation.

The SINR at the receiving end of user i can be expressed as:

$$SINR_i = \frac{\left|\mathbf{h}_i^H \mathbf{t}_i\right|^2}{\sum\limits_{j \neq i}\left|\mathbf{h}_i^H \mathbf{t}_j\right|^2 + N_0 W} = \frac{p_i\left|\mathbf{h}_i^H \mathbf{w}_i\right|^2}{\sum\limits_{j \neq i} p_j\left|\mathbf{h}_i^H \mathbf{w}_j\right|^2 + N_0 W} \tag{2}$$

where N_0 is the noise power spectral density and W is the total bandwidth. Therefore, the maximum achievable Shannon rate of user i is:

$$r_i = W \log_2(1 + SINR_i), \forall i = 1, 2, \ldots, K \tag{3}$$

2.3. High-Throughput Satellite System Channel Model

For the LOS (line of sight) satellite channel with the center frequency above 10 GHz, the performance and availability of the high-throughput satellite system will be greatly reduced due to various atmospheric effects in the troposphere. Among various atmospheric effects, rainfall attenuation is the most critical and dominant factor, especially in the Ka-band. Therefore, the influence of rainfall attenuation should be emphatically considered in modeling. Due to the high frequency of the Ka-band and the excessive free space loss of electromagnetic waves, the transmitting and receiving gain of omnidirectional antennas configured for ground mobile users is not enough to meet the link budget. Therefore, the Ka-band high-throughput satellite system is only suitable for providing fixed user services, and satellite mobile services are generally provided by L-band satellites [13]. In this paper, when establishing the channel model of a high-throughput satellite system, the effects of free space loss, rainfall attenuation, and beam gain are considered at the same time. The channel matrix can be expressed as:

$$H = \widetilde{H}B \tag{4}$$

where the $K \times K$ dimension rainfall attenuation matrix $\widetilde{H}$ simulates the influence of rainfall attenuation, and the $K \times K$ dimension multi-beam antenna gain matrix B simulates the influence of satellite antenna radiation mode, receiving antenna gain, path loss, and noise power.

The size of the multi-beam antenna gain matrix depends on the radiation pattern of the antenna beams and the position of each user terminal antenna in the beam. For a high-throughput satellite communication system providing fixed user services, the multi-beam antenna gain matrix is fixed, whose (i, j) item $b_{i,j}$ can be expressed as:

$$b_{i,j} = \frac{\sqrt{G_R^i G_{i,j}}}{4\pi \frac{\sqrt{d_0^2 + d^2}}{\lambda}\sqrt{\kappa_B T B_W}} \tag{5}$$

where $G_{i,j}$ is the multi-beam antenna gain from the j-th satellite feed to the i-th user terminal, G_R^i is the antenna gain of the user terminal, κ_B is the Boltzmann constant, T is the receiver noise temperature, B_W is the user link bandwidth, λ is the carrier wavelength, d_0 is the distance from the satellite to the user-located beam center, and d is the distance from the ground user terminal to the user-located beam center. Due to the curvature of the earth and the wide-area coverage characteristics of satellites, the introduction of d can more accurately describe the difference of free space loss between different beams of the high-throughput satellite system.

The multi-beam antenna gain $G_{i,j}$ from the j-th satellite feed to the i-th user terminal mainly depends on the radiation mode of satellite transmitting antennas and user position, which can be expressed as:

$$G_{i,j} = G_T^j \left(\frac{J_1(u_{i,j})}{2u_{i,j}} + 36\frac{J_3(u_{i,j})}{u_{i,j}^3} \right)^2 \tag{6}$$

where G_T is the transmit antenna gain, intermediate quantity $u_{i,j} = 2.07123\frac{\sin(\theta_{i,j})}{\sin(\theta_{i,3dB})}$. $\theta_{i,j}$ is the angle of the path from the i-th user to the j-th beam center relative to the satellite, and $\theta_{i,3dB}$ is the 3 dB beam angle of the i-th beam; that is, the beam where the user is. $J_1(\cdot)$ and $J_3(\cdot)$ are the first-order and third-order Bessel functions, respectively.

The method of modeling rainfall attenuation adopts the latest empirical model in the ITU-R P.618 recommendation [14], and the power gain ξ_{dB} in dB follows lognormal distribution, that is, $\ln(\xi_{dB}) \sim N(\mu, \sigma^2)$. μ and σ^2 are the mean and variance of the corresponding normal distribution, respectively, which are related to the receiver position, operating frequency, polarization, and satellite elevation angle. Therefore, the rainfall attenuation matrix $\widetilde{H}$ can be expressed as $\widetilde{H} = diag\left\{\sqrt{\xi_1}e^{-j\varphi_1}, \ldots, \sqrt{\xi_K}e^{-j\varphi_K}\right\}$, where $\sqrt{\xi_k}e^{-j\varphi_k}$ is the rainfall attenuation factor of the k-th user. Since the feed spacing of a multi-beam antenna is much smaller than the signal propagation distance, it is assumed that the rainfall attenuation factor between different beams and the same user is the same, and φ follows a uniformly distributed phase, that is $\varphi \sim U(0, 2\pi)$.

3. Regularized Zero-Forcing Dirty Paper Precoding of a High-Throughput Satellite Communication System

3.1. Zero-Forcing Precoding

Precoding refers to the process of using channel state information to obtain the precoding matrix on the ground gateway side and processing the transmitted signal to reduce interference. The zero-forcing precoding algorithm is the most classical precoding algorithm, whose main idea is to multiply the modulated signal **s** by the inverse matrix of the channel matrix at the transmitting end first. Secondly, the precoding processed signal is transmitted through the channel and finally multiplied by a channel matrix to eliminate the interference between signals. The idea is described in mathematical language and can be equivalent to $\mathbf{HW}_{ZF}=\mathbf{I}$. The precoding matrix is obtained by calculating the pseudo-inverse of the channel matrix. Therefore, the expression of the zero-forcing precoding matrix is:

$$\mathbf{W}_{ZF} = \left(\mathbf{H}^H\mathbf{H}\right)^{-1}\mathbf{H}^H \tag{7}$$

In practical application, the precoding vector of a corresponding user can be obtained by normalizing each column vector in the zero-forcing precoding matrix. It can be seen from the above calculation that the zero-forcing precoding algorithm can eliminate the interference of users in the same frequency. However, without considering the influence of noise, the zero-forcing precoding algorithm is an optimal precoding scheme only when there is no additive noise, and the system performance will be poor in the case of low SNR.

3.2. Regularized Zero-Forcing Precoding

Zero-forcing precoding is asymptotically optimal in the case of high SNR, but it does not consider the impact of channel noise on system performance. Therefore, regularized zero-forcing precoding introduces a regularization parameter considering the influence of noise, and it has good performance in the case of low SNR. The process of the regularized zero-forcing precoding algorithm is basically the same as that of the zero-forcing precoding algorithm; that is, the minimum mean square error criterion is used to calculate the pre-

coding matrix, and the noise and user interference are eliminated by suppressing noise amplification. The expression of the regularized zero-forcing precoding matrix is:

$$\mathbf{W}_{RZF} = \left(\mathbf{H}^H\mathbf{H} + \alpha\mathbf{I}_K\right)^{-1}\mathbf{H}^H \tag{8}$$

It can be seen from Equation (8) that the regularized zero-forcing precoder is essentially a zero-forcing precoder regularized by a regularization factor α. In the case of $\alpha \to \infty$, Equation (8) represents a matched filter. In the case of $\alpha \to 0$, Equation (8) represents a zero-forcing precoder. For a high-throughput satellite system, $\alpha = \frac{N_0 W}{P_0}$, where P_0 is the highest power of the feed. The influence of receiver noise is considered in the calculation process of the regularized zero-forcing precoding matrix. Due to the noise factor, the interference between users cannot be eliminated. However, in the case of low SNR, the performance of regularized zero-forcing precoding is better than that of zero-forcing precoding.

3.3. Dirty Paper Regularized Zero-Forcing Precoding

Dirty paper precoding is considered to be the sum rate capacity realization technology in the MIMO link, as well as the best precoding technology. However, it is often very complicated to determine the optimal coding order and optimal correlation matrix of precoding. Therefore, this paper proposes a low-complexity dirty paper regularized zero-forcing precoding scheme, which is based on the idea of dirty paper precoding to optimize regularized zero-forcing precoding.

In the downlink channel of the high-throughput satellite forward link, different users in different beams can be arranged in descending order according to the strength of channel gain, that is, the channel degradation. When the dirty paper precoding algorithm is implemented, the coding order must be determined first. Therefore, we first face the problem of selecting multiple coding sequences. Generally, the first coded user receives a large amount of interference, and the interference received by the coded user decreases gradually with the progress of serial coding. Therefore, from the technical perspective, users with good channel conditions should be coded first, because they have the ability to withstand interference. Moreover, users with high-rate requirements should be coded last, from the demand perspective, because they must avoid interference to achieve the required rate. Therefore, this paper refers to the principle of channel maximum norm selection and combines with the practical application scenarios to sort users according to the descending order of the defined metrics as $\log_2(1 + \|h_i\|^2)$. The following analysis is generalizable. We assume that when $K = 2$, $\|h_1\|^2 \leq \|h_2\|^2$, the channel conditions of the users in beam 2 are better than those in beam 1, and beam 2 can deal with stronger interference than beam 1. s_1 and s_2 represent the user signals of beam 1 and beam 2, respectively, and the transmitter signal is the superposition of them: $(s_1 + s_2)$. It is assumed that the transmission power of beam 1 and beam 2 is p_1 and p_2, respectively. Considering the idea of dirty paper coding, beam 2 is coded first, and the signal of beam 1 is regarded as an interference signal. At this time, the rate reached can be expressed as:

$$R_2 = \log_2\left(1 + \frac{p_2\left|h_2^H w_2\right|^2}{p_1\left|h_2^H w_1\right|^2 + N_0 B_W}\right) \tag{9}$$

After coding for the user in beam 2, the user in beam 1 is precoded by means of successive interference cancellation, and the achievable user rate can be expressed as:

$$R_1 = \log_2\left(1 + \frac{p_1\left|h_1^H w_1\right|^2}{N_0 B_W}\right) \tag{10}$$

Extending the situation of the above two beams to the actual satellite communication system, the application flow chart of dirty paper regularized zero-forcing precoding can

be expressed as Figure 3, where the precoding vector w_i is obtained by the regularized zero-forcing precoding.

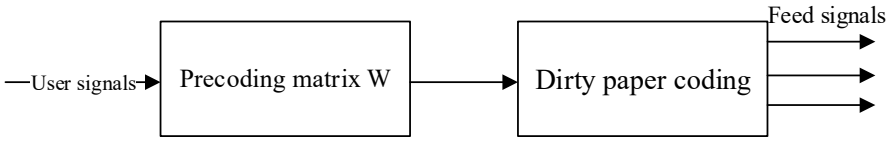

Figure 3. Application flow chart of dirty paper regularized zero-forcing precoding.

After obtaining the coding order, the achievable SINR of the *i*-th user can be expressed as:

$$\Gamma_i = \frac{p_i \left| \mathbf{h}_i^H \mathbf{w}_i \right|^2}{\sum_{j>i} p_j \left| \mathbf{h}_i^H \mathbf{w}_j \right|^2 + N_0 W} \tag{11}$$

For the user in the *i*-th beam, the achievable user rate can be expressed as:

$$R_i = W \log_2(1 + \Gamma_i) \tag{12}$$

4. Simulation Verification and Analysis

Simulation analysis is carried out to verify the performance of several precoding algorithms described in this paper. The simulation parameters of the high throughput satellite communication system are shown in Table 1. Because the achievable rate of users is different when different precoding schemes are adopted, the maximum beam power of each feeder is defined to be 80 W, and 7 feeders are used to form 7 beams on the satellite. Currently, in the TDMA communication mode, each beam has one user communicating in the transmission time slot, and we can select a user from each beam to form a group of 7 users to design the precoding matrix. The method of selecting users in the same time slot is an important factor affecting the overall performance of the system, so the influence of user arrangement in the beam on system performance will also be considered in the simulation and analysis.

Table 1. Parameters of a high throughput satellite communications system.

Parameter	Value
Orbit	Geostationary orbit
Carrier frequency (GHz)	20
Number of beams	7
Coverage area diameter (km)	500 km
3 dB angle	0.4
Mean of rainfall attenuation (dB)	0.6
Variance of rainfall attenuation (dB)	1
Polarization mode	Single-polarization
Maximum antenna transmitting gain (dBi)	50
User terminal receiving gain (dBi)	45
Free space loss of forward link (dB)	210
User link bandwidth (MHz)	500
Noise temperature of receivers (K)	207
Distribution of user terminals	Fixed

Since the greatest feature of a high-throughput satellite is its high throughput, in this paper, the throughput is used to describe the performance of a high-throughput satellite system in the simulation. The throughput of the *i*-th beam can be expressed by SINR:

$$C_i = W \log_2(1 + SINR_i) \tag{13}$$

where $SINR_i$ is the SINR of the i-th user at the receiving end, which is defined by Equation (2). The average throughput of the system is the average of all beam throughputs. In addition, the traditional satellite system usually selects the four-color frequency reuse scheme; therefore, the adjacent beams use different frequency bands to reduce the interference. Therefore, this scheme is also considered in the simulation to compare and show the improvement effect of the precoding algorithm on system throughput. The maximum achievable throughput of each beam under the four-color frequency reuse scheme can be expressed as:

$$C_i = \frac{W}{4} \log_2 \left(1 + \frac{4 p_i |h_{i,i}|^2}{N_0 W} \right) \tag{14}$$

Figure 4 shows the simulation of the throughput performance of three precoding schemes, including zero-forcing, regularized zero-forcing, and regularized zero-forcing dirty paper precoding, as well as the four-color frequency reuse scheme. When the regularized zero-forcing dirty paper precoding is used, the user channel corresponding to 7 beams should be sorted first, so the simulated beam number is the sequence after the channel maximum norm selection. It can be seen that although the traditional frequency reuse mode does not have serious co-frequency interference problems, its available bandwidth is only a fraction of the full spectrum reuse satellite system, and its achievable throughput is significantly lower than that of the full spectrum reuse satellite system. Three precoding algorithms, including zero-forcing, regularized zero-forcing, and regularized zero-forcing dirty paper precoding can improve the SINR and obtain the throughput at several times the available bandwidth; thus, they can better eliminate interference. Compared with the zero-forcing precoding algorithm, regularized zero-forcing precoding reduces the amplification of noise, and its achievable throughput is increased by about 5%. Moreover, the regularized zero-forcing dirty paper precoding algorithm can achieve the largest throughput, which is further improved by about 5% compared with regularized zero-forcing precoding.

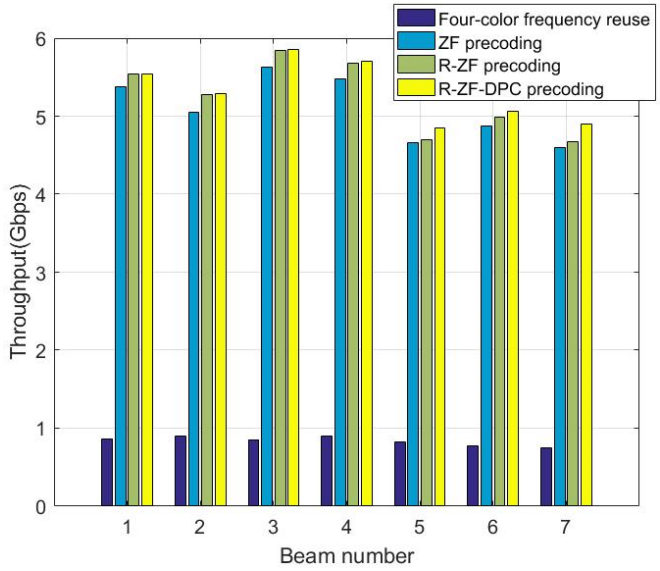

Figure 4. Performance diagram of each beam throughput of four precoding schemes.

Figure 5 is the comparison of the influence of beam number on the throughput per beam of four precoding schemes. A random order regularized zero-forcing dirty paper precoding algorithm is added, which aims to reduce the complexity and analyze its advantages and disadvantages. It can be seen that the average achievable throughput of all four precoding schemes decreases with the increase in the number of beams. Especially in the process of changing the number of beams from 7 to 19 to 37, the decreasing trend is obvious because the increased number of beams will bring more co-channel interference.

The average beam throughput of zero-forcing precoding is most affected by the increase in the number of beams because it does not consider the suppression of the noise in the system. With the increase in the number of beams, the noise in the system is greater, and the impact is more prominent. The other three precoding schemes are basically the same, as they are affected by the increase in the number of beams, and the regularized zero-forcing dirty paper precoding scheme with a determined coding sequence has the best performance.

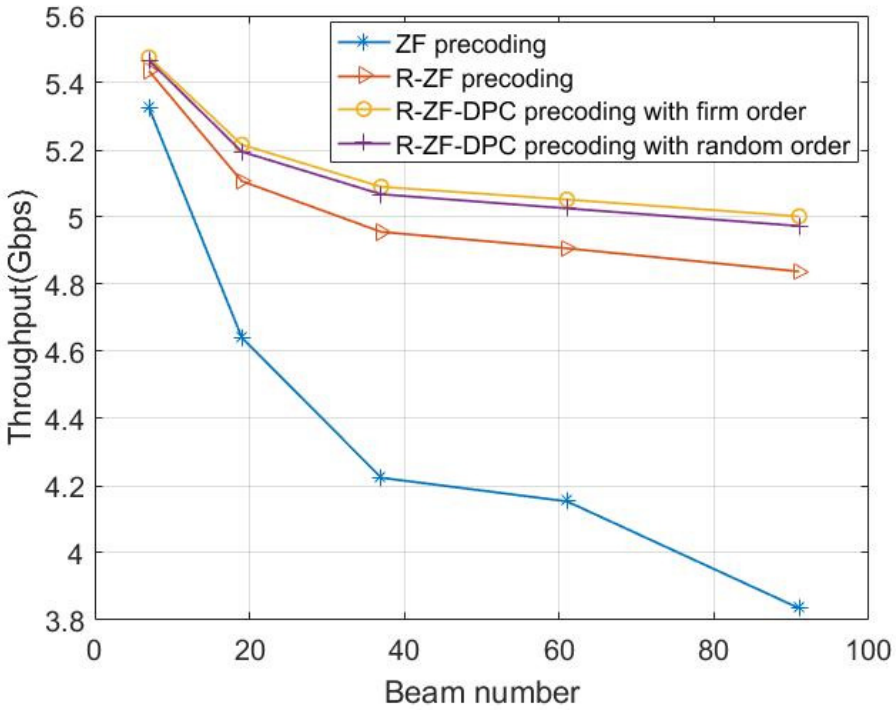

Figure 5. Influence of beam number on throughput per beam of four precoding schemes.

Figure 6 shows the influence of the 3 dB angle on the throughput performance of the precoding schemes with random user location. It can be seen that in a certain range of beam coverage, given the beam radius, when the 3 dB angle of the beam increases, the system's achievable throughput increases first and then decreases, and the maximum extreme point is the edge of the beam, which is a 3 dB power attenuation. It can be concluded that when selecting the beam coverage form, it is best to select the 3 dB beam width as the beam edge. Moreover, it is found that the performance of the regularized zero-forcing dirty paper precoding algorithm is the best, as it is far less affected by the 3 dB angle than is the zero-forcing precoding, and there is little difference between the performance of the two dirty paper regularized zero-forcing precoding algorithms with two coding sequences.

Figure 7 shows the influence of 3 dB angle on throughput performance of precoding schemes with users distributed at the edge of the beam. In the satellite communication system, the performance of the worst external conditions should be considered when measuring the system performance; in other words, the situation where users are distributed at the edge of the beam. It can be seen that when users are arranged at the edge of the beam and the 3 dB angle of the beam is small, the achievable throughput of the system is much different from that with a random user arrangement. However, when the 3 dB width of the beam exceeds the beam diameter, the user arrangement basically does not affect the system throughput performance.

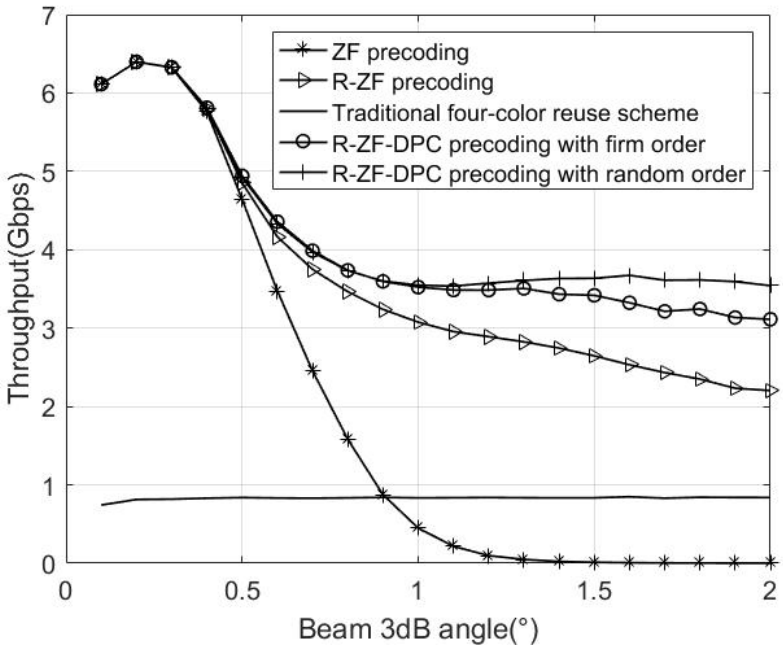

Figure 6. Influence of the 3 dB angle on the throughput performance of precoding schemes with random user location.

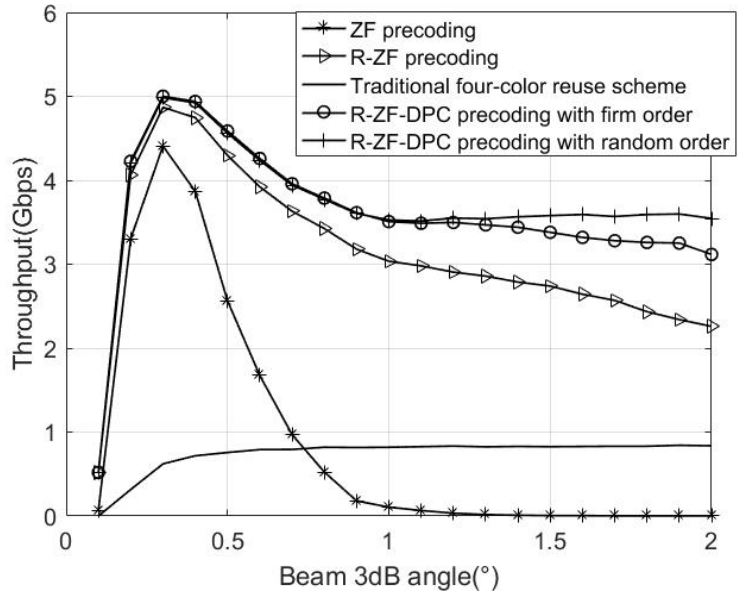

Figure 7. Influence of 3 dB angle on throughput performance of precoding schemes with users distributed at the edge of the beam.

Figure 8 shows the influence of the size of the beam overlap area on the system performance with random user location. The overlap factor is defined as the ratio of the beam radius to the radius when there is no overlap between beams. It is assumed that the edge power attenuation of each beam is 3 dB, and the beam center position is given. It can be seen that when there is no beam overlap and the user random distribution model is adopted, the achievable throughput performance curves of the four precoding schemes basically coincide. When the beam overlap factor is larger than 1.2, the performance of the zero-forcing precoding algorithm decreases significantly.

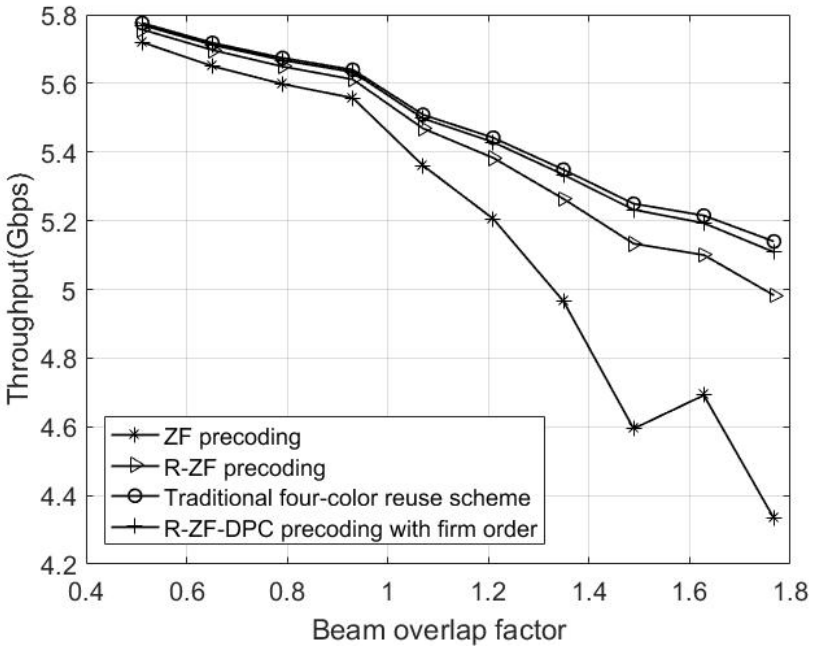

Figure 8. Influence of overlap factor on throughput performance of precoding schemes with random user location.

Figure 9 shows the influence of the size of the beam overlap area on the system performance with users distributed at the edge of the beam. It can be seen that when users are distributed at the edge of the beam and the beam overlap factor is small, the throughput performance of the beam will decrease more obviously with the increase in the overlap factor. When the beam overlap factor is large, the beam throughput performance changes slightly with the increase in overlap factor; thus, it tends to be stable. Additionally, the achievable throughput of users distributed at the edge of the beam is less than that of the random user distribution model under the same overlap factor.

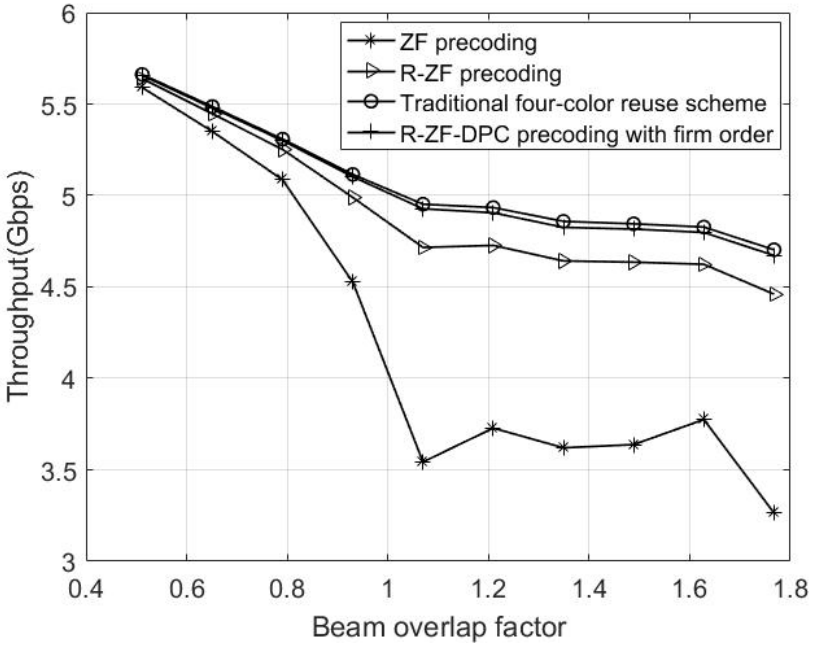

Figure 9. Influence of overlap factor on throughput performance of precoding schemes with users distributed at the edge of the beam.

5. Conclusions

This paper studies the precoding problem of the high-throughput satellite forward link. Based on the forward link model, considering the effects of free space loss, rainfall attenuation, and beam gain, the classical low-complexity zero-forcing precoding algorithm is improved in this paper. Moreover, the regularized zero-forcing precoding algorithm considering the influence of system noise is studied, and a low complexity regularized zero-forcing dirty paper precoding algorithm is proposed, based on the idea of continuous interference elimination using non-linear dirty paper coding to achieve the maximum rate. It can be seen through simulation analysis that the throughput of regularized zero-forcing dirty paper precoding is larger, and the greater the number of formed beams, the worse the throughput performance per beam. The beam edge at 3 dB width shows the best performance. When the beam overlap factor exceeds a certain extent, the regularized zero-forcing dirty paper precoding algorithm is more robust than other algorithms. It can be concluded that the proposed dirty paper regularized zero-forcing precoding, which introduces the idea of dirty paper coding, can achieve better performance than classical precoding algorithms.

Author Contributions: Conceptualization, M.Y.; methodology, M.Y.; software, X.S.; validation, X.S., G.X. and B.L.; investigation, B.L.; resources, G.X.; data curation, X.S.; writing—original draft preparation, G.X.; writing—review and editing, Y.S.; visualization, G.X.; supervision, M.Y.; funding acquisition, M.Y. All authors have read and agreed to the published version of the manuscript.

Funding: This research was funded by National Natural Science Foundation of China, grant number No.62071146.

Data Availability Statement: The data presented in this study are available on request from the corresponding author.

Conflicts of Interest: The authors declare no conflict of interest.

References

1. Guidotti, A.; Vanelli-Coralli, A. Clustering strategies for multicast precoding in multibeam satellite systems. *Int. J. Satell. Commun. Netw.* **2020**, *38*, 85–104. [CrossRef]
2. Costa, M. Writing on dirty paper (Corresp.). *IEEE Trans. Inf. Theory* **1983**, *29*, 439–441. [CrossRef]
3. Yoo, T.; Goldsmith, A. On the optimality of multiantenna broadcast scheduling using zero-forcing beamforming. *IEEE J. Sel. Areas Commun.* **2006**, *24*, 528–541.
4. Cottatellucci, L.; Debbah, M.; Gallinaro, G.; Mueller, R.; Neri, M.; Rinaldo, R. Interference mitigation techniques for broadband satellite systems. In Proceedings of the 24th AIAA International Communications Satellite Systems Conference, San Diego, CA, USA, 11–14 June 2006; pp. 2–15.
5. Devillers, B.; Pérez, N.; Isabel, A.; Mosquera, C. Joint linear precoding and beamforming for the forward link of multi-beam broadband satellite systems. In Proceedings of the Global Telecommunications Conference, Houston, TX, USA, 5–9 December 2011; IEEE: Piscataway, NJ, USA, 2012.
6. Tronc, J.; Song, N.; Haardt, M.; Arentd, J.; Gallinaro, G. Overview and comparison of on-ground and on-board beamforming techniques in mobile satellite service applications. *Int. J. Satell. Commun. Netw.* **2014**, *32*, 291–308. [CrossRef]
7. Maturo, N.; Duncan, J.; Krivochiza, J.; Querol, J.; Spano, D.; Chatzinotas, S.; Ottersen, B. Demonstrator of precoding technique for a multi-beams satellite system. In Proceedings of the 2019 8th International Workshop on Tracking, Telemetry and Command Systems for Space Applications (TTC), Darmstadt, Germany, 24–27 September 2019.
8. Ahmad, I.; Nguyen, K.D.; Letzepis, N.; Lechner, G.; Joroughi, V. Zero-forcing precoding with partial CSI in multibeam high throughput satellite systems. *IEEE Trans. Veh. Technol.* **2021**, *70*, 1410–1420. [CrossRef]
9. Mysore, B.; Lagunas, E.; Chatzinotas, S.; Ottersten, B. Precoding for satellite communications: Why, how and what next. *IEEE Commun. Lett.* **2021**, *25*, 2453–2457. [CrossRef]
10. Panagopoulos, A.; Arapoglou, P.; Cottis, P. Satellite communications at KU, KA, and V bands: Propagation impairments and mitigation techniques. *IEEE Commun. Surv. Tutor.* **2004**, *6*, 2–14. [CrossRef]
11. Isabona, J.; Imoize, A.; Ojo, S.; Lee, C.; Li, C. Atmospheric Propagation Modelling for Terrestrial Radio Frequency Communication Links in a Tropical Wet and Dry Savanna Climate. *Information* **2022**, *13*, 141. [CrossRef]
12. Al-Saegh, A.; Sali, A.; Mandeep, J.; Ismail, A.; Al-Jumaily, A.; Gomes, C. Atmospheric Propagation Model for Satellite Communications. In *MATLAB Applications for the Practical Engineer*; Bennet, K., Ed.; InTech: London, UK, 2014.

13. Guidotti, A.; Vanelli-Coralli, A. Design Trade-Off Analysis of Precoding Multi-Beam Satellite Communication Systems. In Proceedings of the IEEE Aerospace Conference, Big Sky, MT, USA, 6–13 March 2021; IEEE: Piscataway, NJ, USA, 2021.
14. Series, P. *Propagation Data and Prediction Methods Required for the Design of Earth-Space Telecommunication Systems*; Recommendation ITU-R, 618–12; ITU: Geneva, Switzerland, 2015.